Hindawi
Advances in Civil Engineering
Volume 2018, Article ID 7569578, 12 pages
https://doi.org/10.1155/2018/7569578

Research Article

Effect of Loading Direction and Slope on Laterally Loaded Pile in Sloping Ground

Chong Jiang, Jia-Li He, Lin Liu, and Bo-Wen Sun

School of Resources and Safety Engineering, Central South University, Changsha 410083, Hunan, China

Correspondence should be addressed to Chong Jiang; jiang4107@sohu.com and Lin Liu; liulin9358@csu.edu.cn

Received 11 September 2018; Accepted 25 October 2018; Published 15 November 2018

Guest Editor: Xihong Zhang

A series of three-dimensional finite element analyses were performed to study the behavior of piles in sloping ground under undrained lateral loading conditions. The analyses have been conducted for slopes with different angles and two loading directions. The obtained results show that as the slope increases, it can cause greater lateral displacement and internal force of the pile. In addition, the increase of the slope ratio will cause the position of the maximum bending moment and soil resistance zero point of the pile to move downward, further increasing the pile deflection. Furthermore, when the pile distance from slope crest $B < 7D$, the displacement and internal force development of the pile under toward loading is more obvious. When the pile distance from the slope crest exceeds $7D$, the effect of loading direction on the pile can be neglected.

1. Introduction

Pile foundations are widely used to support structures such as bridges, high-rise buildings, and transmission towers, and they are often constructed on a natural or artificially constructed slope. Pile foundations are often subjected to lateral loads caused by wind and earthquakes. When the foundation is built on a slope, the bearing capacity of the foundation will be significantly reduced, depending on the distance of the foundation from the slope. The bearing capacity of the foundation on the slope is usually calculated by empirical or theoretical formulas which are based on the limit equilibrium or the upper boundary plasticity calculation. For the design of pile foundations subjected to lateral loads, the lateral response of the piles on the slopes and the interaction of piles with the soil are of great importance.

In order to obtain the design method and related theoretical guidance of the laterally loaded pile foundation on the slope site, some scholars have tried to study in theory and put forward some optimization design methods [1–3]. At present, many research scholars have carried out field tests [4–6] and laboratory tests [7, 8] on laterally loaded pile foundations on slope sites. In order to study the influence of slope on the pile foundation, Mezazigh and Levacher [9] carried out a centrifuge model test of the laterally loaded pile in the nonadhesive soil foundation. According to the curve distribution results under different working conditions in the test, the slope was applied to the shallow nonadhesive soil foundation. Based on the model test of piles in noncohesive soil slopes, Muthukkumaran [10] discussed the effects of slope ratio, soil parameters, loading direction, and pile foundation position on pile foundation. Nimityongskul et al. [11] carried out a series of full-scale lateral load tests of fully instrumented piles in cohesive soils to access the lateral response of piles in free field and near a slope condition.

More and more scholars choose numerical simulation to analyze the problem of actual pile-soil interaction [12–14]. Zhang et al. [15] established a three-dimensional calculation model based on the actual situation of the slope engineering in Hong Kong. Through numerical calculation and analysis, the influence of slope and casing thickness on the performance of the laterally loaded pile foundation on the slope was discussed. A large-scale commercial finite element software was used by Georgiadis and Georgiadis [13] to establish a three-dimensional model to study the nonlinear response behavior of piles in sloping ground under

undrained lateral loading conditions. Two parameters of slope ratio and soil shear strength were selected for sensitivity analysis under different working conditions. Based on the calculation results, the curve in the form of hyperbolic curve is modified to consider the influence of slope ratio and the cohesion coefficient of the pile-soil cross section. Finally, the feasibility of the proposed method is verified by an example check. Through the three-dimensional finite element model, the influence of the laterally loaded pile foundation on the bearing performance of the pile foundation is studied by Sawant and Shukla [16].

To sum up, the current study on laterally loaded piles on slope sites is mainly based on model tests. Some scholars have used numerical software to simulate and obtain some research results on slope effects. However, there is currently no detailed analysis of factors' impact on slopes. Therefore, this paper will use the finite element software to establish the geometric calculation model of the laterally loaded pile on the slope site, calculate, and analyze the deformation of the pile. In the simulation analysis, the influences of slope ratio and loading direction on the displacement of laterally loaded piles, internal forces, and soil resistance of piles are studied so as to further reveal and summarize the bearing characteristics of laterally loaded single piles on slope sites and to provide reference for practical engineering design and optimization.

2. Numerical Simulation

2.1. Finite Element Model. A circular pile foundation with a length of 12 m and a diameter of 1 m was located near the slope. In order to avoid the influence of size effect on the calculation results, the length of the slope top and the whole width of the model were 20 times the pile diameter. The height of the slope was 12 m, and the total height of the model was 2 times the length of the pile. It was assumed that the pile foundation and soil are isotropic homogeneous materials, and Poisson's ratio and elastic modulus did not change with the load. The top boundary of the model was free. The four vertical sides of the model set the radial displacement constraint; that is, U2 = 0 was set on the front and back sides and U1 = 0 was set on the left and right sides. The bottom surface of the model was set as the fixed boundary, whereas the top surface of the pile remained free. In the mesh generation of this model, the eight-node hexahedron linear reduced element was used to simulate the pile foundation and soil. The grid around the contact surface between pile foundation and soil should be subdivided, and the grid setting proportion away from the contact surface gradually evacuated. The grid of the pile foundation and soil mass in the slope calculation model is shown in Figure 1.

The main process of numerical modeling is as follows:

(1) In order to balance the initial stress, the model of a pile foundation in a slope was established, and the original soil at the pile hole was preserved. A gravity value of −10 in the Z direction was applied to the entire soil model (opposite to the Z-axis direction). The geostatic automatic stress balance method was used to calculate the original initial stress field of the slope.

(2) After the initial stress calculation of the slope soil was completed, the "model change" function was used to kill the soil at the pile hole, and the pile foundation component was modified into a living unit to reactivate the pile foundation.

(3) A contact pair was added to the contact faces of the pile body, the pile end, and the soil body, respectively. Then, the self-weight value of −10 in the Z direction was applied to the pile foundation so that the pile foundation interacted with the slope soil under the action of self-weight until equilibrium.

Different loading steps were established to apply lateral loads on the pile head step by step.

2.2. Verification of the Numerical Model. Georgiadis and Georgiadis [13] performed three-dimensional finite element analyses to study the behavior of piles in sloping ground under undrained lateral loading conditions. The numerical simulation results of the model in this paper were compared with those in the literature to verify the rationality of the model. The pile foundation parameters were set as follows: pile length L = 12 m, pile diameter D = 1 m, and slope angle = 30°. The soil and pile properties of the three-dimensional finite element model are shown in Table 1.

In the contact setting, the normal behavior was set to the "hard" contact mode, and the tangential behavior was in the form of "penalty" friction. The "penalty" friction coefficient value μ was generally 0.36 (tan(0.75φ)), and the case where the contact surface of the pile and soil was completely rough was considered, so μ = 1. In particular, the stability of slope must be ensured before the three-dimensional calculation of the laterally loaded piles in sloping ground. The stability of the slope is not taken into consideration, and the pile foundation does not play the role of an antislide pile but serves to the bearing structure. Therefore, according to the soil and pile properties, the slope stability calculation formula and chart given by Taylor were used for analysis [17]. The slope safety factor of the model was calculated to exceed 1.08, which proved that the slope was stable.

The comparative results of the model in this paper and the 3D finite element analyses are shown in Figure 2. A good compatibility could be seen between the present simulation model and the results of published data. The maximum error is 9.2%, which is within the reasonable error range. It also proves the correctness of the modeling method.

2.3. Type of Analysis. A series of numerical models were performed for various slope angles and loading directions. According to the geological environment conditions in the actual project, the clay will adopt the common c-φ hard clay in the subsequent analysis model. The pile foundation parameters were set as follows: pile length L = 12 m, pile diameter D = 0.6 m, and the material was C30 concrete. The schematic of the model analyzed is presented in Figure 3.

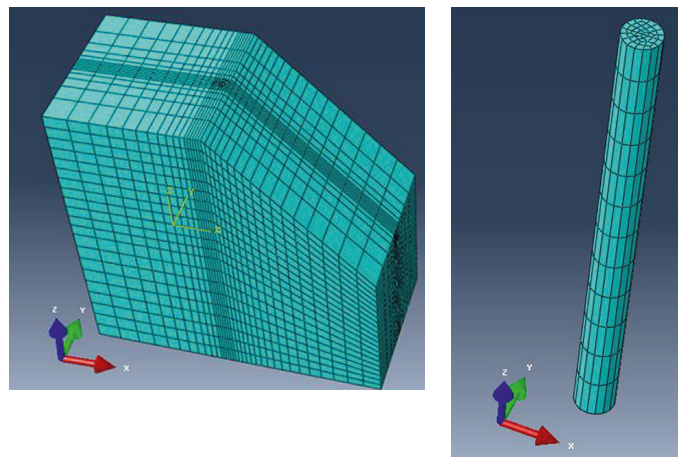

(a) (b)

Figure 1: Typical mesh for three-dimensional finite element analyses. (a) Mesh for soil. (b) Mesh for pile.

Table 1: Soil and pile properties for verification.

	E (Pa)	μ	ρ (kg/m^3)	C (Pa)	φ (°)	ψ (°)
Pile	2.9×10^{10}	0.1	2500	—	—	—
Clay	1×10^7	0.49	1800	5×10^4	0	0

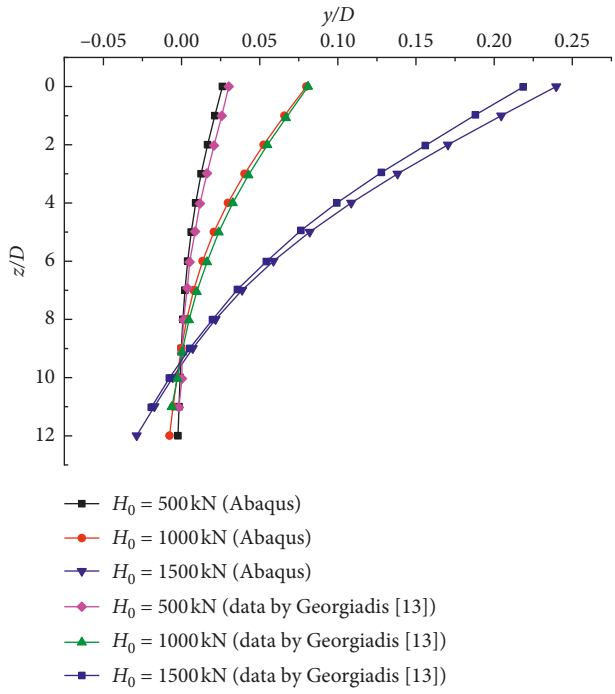

Figure 2: Displacement curve for comparison.

Soil and pile properties used in the finite element analyses are summarized in Table 2.

3. Results and Discussion

3.1. Effect of Slope Ratio. The slope ratio of different models was set as 1V : 1H, 2V : 3H, 1V : 2H, and 1V : 4H,

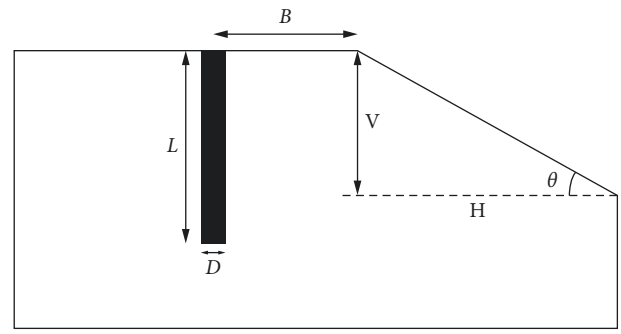

Figure 3: Schematic of the model.

Table 2: Soil and pile properties for modeling.

	E (Pa)	μ	ρ (kg/m^3)	C (Pa)	φ (°)	ψ (°)
Pile	3.0×10^{10}	0.1	2500	—	—	—
Clay	1.2×10^7	0.4	1800	3.0×10^4	35	5

respectively, with the pile distance from slope crest $B/D = 1$. Figure 4 shows the contours of lateral displacement of the pile and soil for the 1V : 1H slope when the lateral load applied on the slope model is 500 kN and 1000 kN, respectively. It can be seen from the figure that both the deflection of the pile and the deformation of the soil before the pile increase with the increase of lateral load. Moreover, the displacement field of the soil in the shallow foundation is distributed in the shape of wedge, which is in good agreement with the assumed shape of the strain wedge model proposed by Xu et al. [18]. The deflection of the pile and the displacement of the wedge mainly occur above a critical position of the pile. Below the critical depth, the pile has an "insertion effect" and the embedded position decreases with the increase of the lateral load.

The pile head load-displacement curves are shown in Figure 5 for different slope ratios. As expected, under the same lateral load H_0, the pile head displacement increases with the increase in the slope ratio. It is clear that the

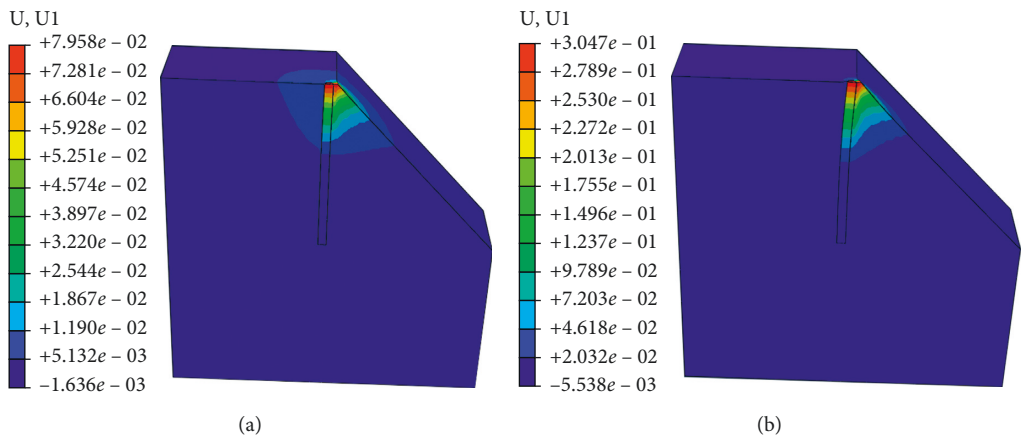

Figure 4: Lateral displacement field at different lateral loads for the 1V : 1H slope. (a) Lateral load H_0 = 500 kN. (b) Lateral load H_0 = 1000 kN.

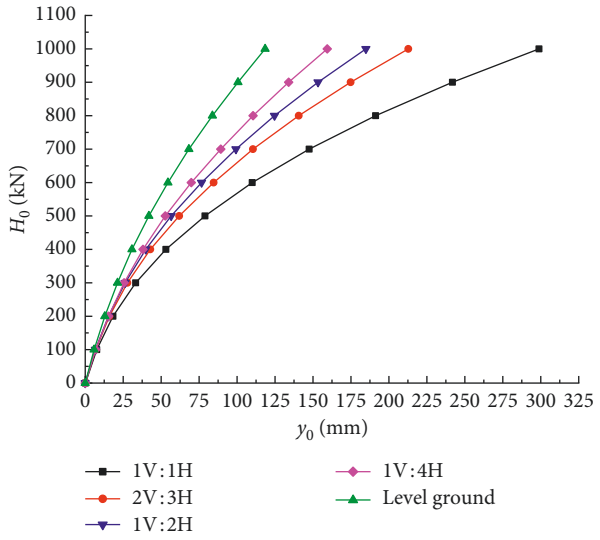

Figure 5: Pile head load-displacement curves for different slope ratios.

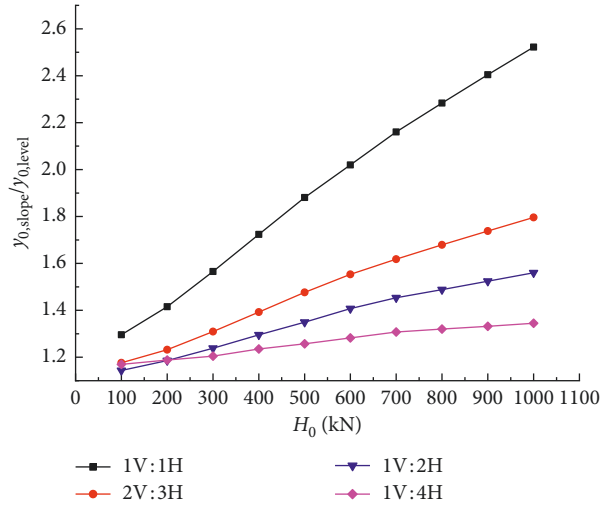

Figure 6: Curves of normalized displacement and lateral load for different slope ratios.

increase in pile head displacement due to slope ratio is larger at higher lateral load.

In order to reflect the effect of the slope ratio on the displacement of the pile head more intuitively, the load-displacement curves in Figure 5 were normalized to obtain the relationship between the normalized displacement $y_{0,slope}/y_{0,level}$ and the lateral load H_0 for different slope ratios. The dimensionless parameter $y_{0,slope}/y_{0,level}$ is defined as the ratio of the displacement of the pile head in sloping ground to the displacement of the same pile head in level ground at the same load levels.

As shown in Figure 6, the normalized displacement value $y_{0,slope}/y_{0,level}$ continues to increase with the increase of lateral load, but the growth rate of $y_{0,slope}/y_{0,level}$ changes as the slope ratio increases. Before the third-stage load, the growth of $y_{0,slope}/y_{0,level}$ is relatively stable for slope ratios of 1V : 4H, 1V : 2H, and 2V : 3H, which is basically between 1.14 and 1.31. However, the growth rate of $y_{0,slope}/y_{0,level}$ increases slowly after the third-level load. The corresponding growth rates in the whole loading process are 14.9%, 36.4%, and 52.7% for slope ratios of 1V : 4H, 1V : 2H, and 2V : 3H, respectively. In contrast, $y_{0,slope}/y_{0,level}$ increases at a fast rate for the 1V : 1H slope ratio throughout the whole loading process, varying from 1.29568 (first-stage load) to 2.52214 (tenth-order load), which increases 94.66%. It indicates that the effect of slope on lateral pile displacement is much larger as the slope gets steeper.

Figures 7 and 8 show the variation of lateral pile deflection with depth for different slope ratios at lateral loads of 500 kN and 1000 kN, respectively. The findings from Figures 7 and 8 can be listed as follows:

(1) The effect of slope ratio is to increase pile deflection at the same load level, and the growth rate of the pile deflection for the 1V : 1H slope ratio is the fastest. Moreover, the increase of pile deflection will become greater as the load level increases.

(2) The pile deflection will increase as the lateral load level increases, which is more obvious in shallow soil layers. Below the position of the first displacement zero point, the pile deflection no longer changes, which is called the "insertion effect."

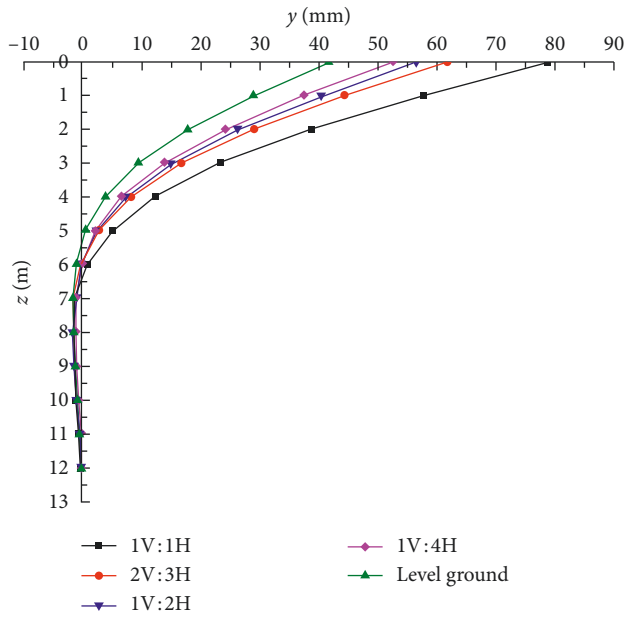

Figure 7: Pile deflection versus depth relationships of different slope ratios for H_0 = 500 kN.

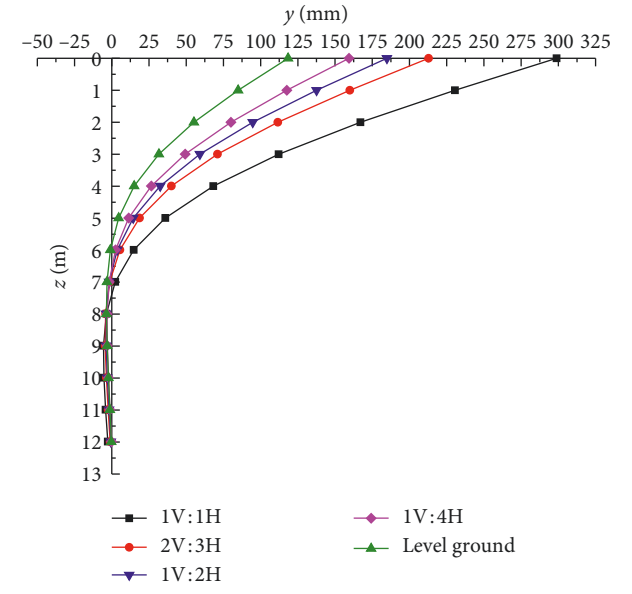

Figure 8: Pile deflection versus depth relationships of different slope ratios for H_0 = 1000 kN.

(3) The increase of the slope ratio will cause the first displacement zero points of the pile to move downward. For example, when the lateral load H_0 = 500 kN, the first displacement zero points for the slope ratios of 1V : 1H, 2V : 3H, 1V : 2H, and 1V : 4H and the level ground appear at 6.5 m, 6.1 m, 5.9 m, 5.86 m, and 5.5 m below the ground surface, respectively.

(4) The shape of pile deflection curves does not change due to the slope effect. However, as the slope ratio increases, the decrease of the soil resistance around the pile will increase the pile deflection at the same depth.

The variation of bending moment with depth for different slope ratios at lateral loads of 500 kN and 1000 kN is presented in Figures 9 and 10, respectively. From Figures 9 and 10, three findings can be drawn:

(1) The slope effect does not affect the shape of the bending moment curves of the pile. The bending moment grows rapidly from 0 on the ground surface to the maximum value and then decreases. There will be two zero points in the bending moment curves of the pile.

(2) The lateral load level affects the position of the maximum bending moment of the pile. When the lateral load H_0 = 500 kN, the positions of maximum bending moment for the slope ratios of 1V : 1H, 2V : 3H, 1V : 2H, and 1V : 4H and the level ground appear at 3.25 m, 3.01 m, 2.92 m, 2.79 m, and 2.71 m below the ground surface, respectively. When the lateral load increases to 1000 kN, the corresponding positions of maximum bending moment appear at 4.28 m, 3.61 m, 3.48 m, 3.25 m, and 2.98 m below the ground surface, respectively. It can be seen that as the load increases, the position of maximum bending moment of the pile will move downward.

(3) The bending moment of the pile increases with the increase of the slope ratio at the same depth. It demonstrates that the elastic deformation range of the pile body is larger and the flexural properties of the pile are more fully developed as the slope ratio increases.

Figure 11 shows the variation in maximum bending moment with the applied lateral load for different slope ratios. In the initial stage of loading, the maximum bending moment is almost the same, indicating that the resistance of the soil around the pile at the stage of elastic deformation is sufficient to balance the maximum bending moment of the pile. When the load exceeds 200 kN, the maximum bending moment of the pile for different slope ratios increases rapidly at different rates. When the lateral load H_0 = 1000 kN, the maximum bending moment of the pile for the slope ratios of 2V : 3H, 1V : 2H, and 1V : 4H is 15.75%, 28.2%, and 38.76%, respectively, higher than that for level ground. The maximum bending moment of the pile for the slope ratio of 1V : 1H is 69.6% higher than that for level ground, which is much higher than the corresponding increase rate for other slope ratios. It indicates that the growth rate of maximum bending moment is much larger with the increase of lateral load as the slope gets steeper.

In order to analyze the effect of slope on the lateral soil resistance, the "free body cut" postprocessing function from the finite element software was used to obtain the data of shear force (Q) of the pile varying with depth. A sixth-order polynomial function has been chosen for the curve fitting in order to reduce the error:

$$Q(z) = az^6 + bz^5 + cz^4 + dz^3 + ez^2 + fz + g. \quad (1)$$

Based on Equation (2), the shear force (Q) versus depth (z) figures were differentiated to give figures of lateral soil

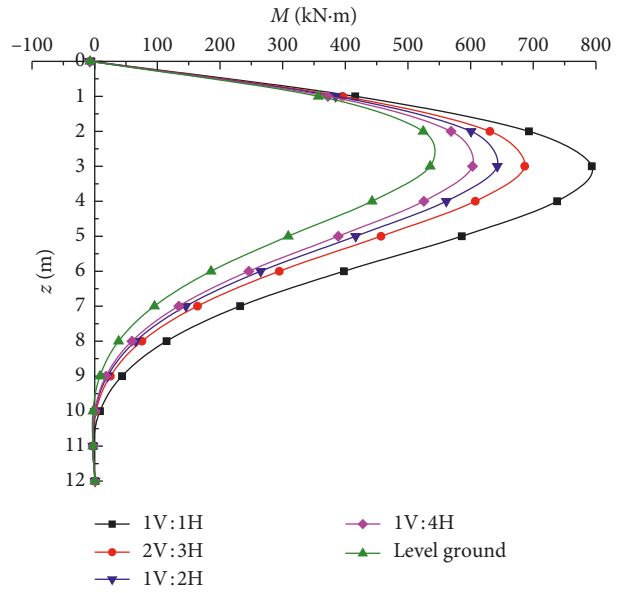

Figure 9: Bending moment of the pile versus depth relationships of different slope ratios for H_0 = 500 kN.

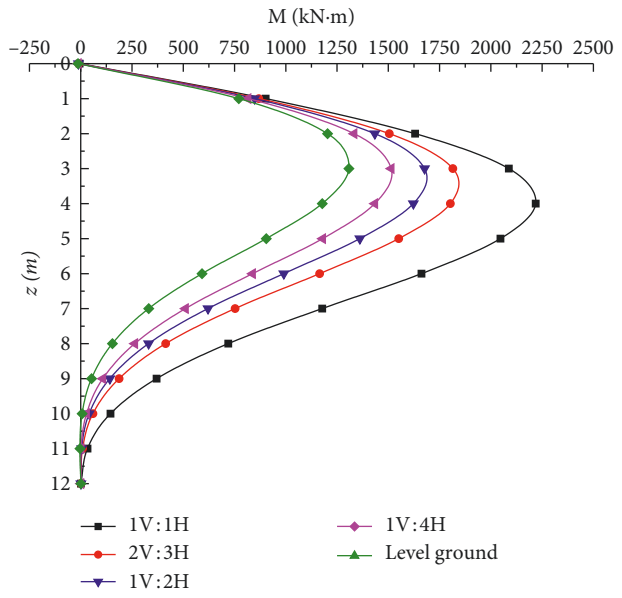

Figure 10: Bending moment of the pile versus depth relationships of different slope ratios for H_0 = 1000 kN.

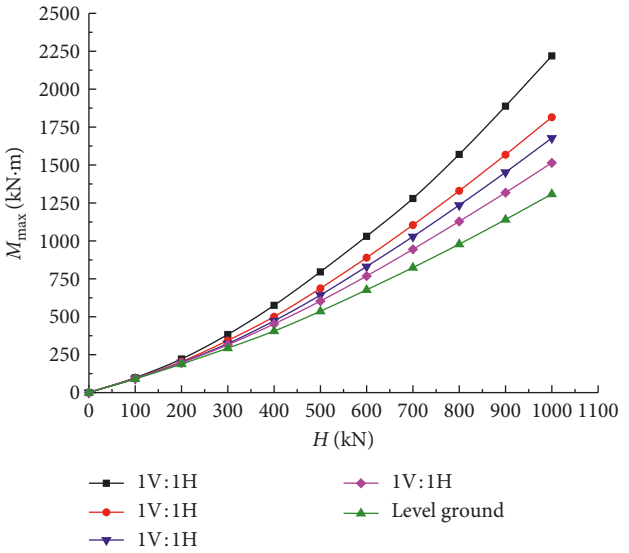

Figure 11: Effect of slope ratio on maximum bending moment.

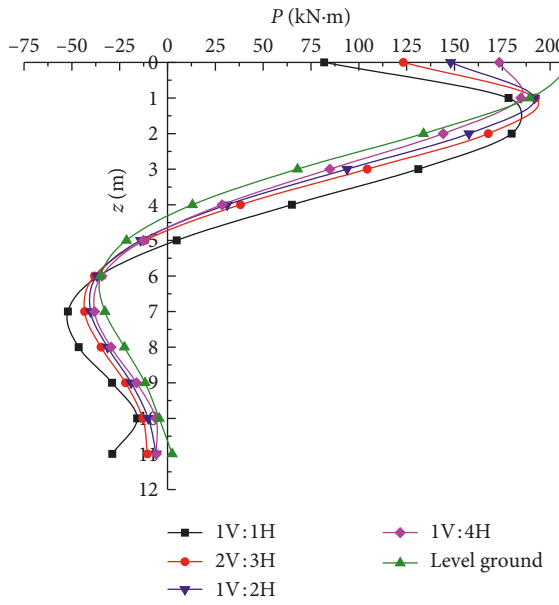

Figure 12: Lateral soil resistance versus depth relationships of different slope ratios for H_0 = 500 kN.

resistance (p) versus depth (z) for different values of pile head load H_0, such as those presented in Figures 12 and 13:

$$p(z) = \frac{dQ(z)}{dz}. \quad (2)$$

The findings from Figures 12 and 13 can be listed as follows:

(1) The shape of the lateral soil resistance curves of the pile in sloping ground is similar to that in level ground. The soil resistance increases from a certain value on the ground surface to the maximum value and then decreases. After reaching the position of the first soil resistance zero point, it increases to the maximum value in the opposite direction. The compressive stress occurs in the soil before the pile above the first soil resistance zero point, while the tensile stress appears in the soil below the point, which is consistent with the direction of the pile deflection.

(2) On the ground surface, the soil resistance will decrease as the slope ratio increases. The soil resistance on the ground surface under level ground condition is the largest. As it was mentioned, the pile head displacement will increase as the slope ratio increases. It can be inferred that when the pile is in level ground and with small slope ratio, the soil resistance is larger in the shallower ground because

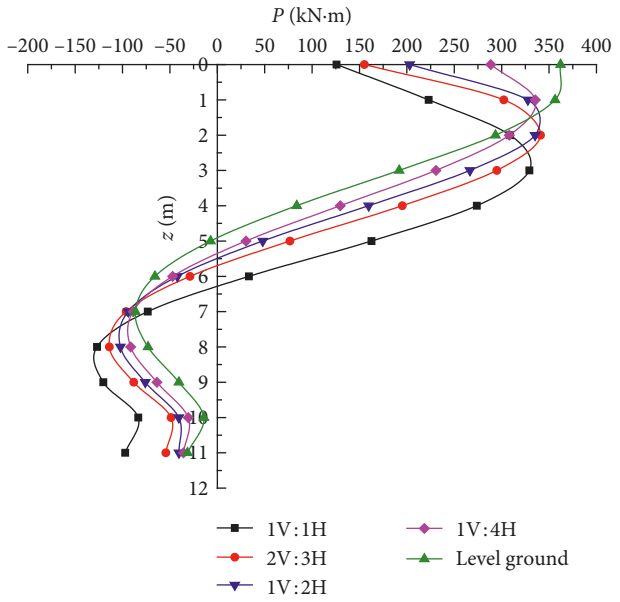

Figure 13: Lateral soil resistance versus depth relationships of different slope ratios for H_0 = 1000 kN.

it is under larger confinement and exposed by smaller pile displacement.

(3) The slope ratio affects the position of the soil resistance zero point of the pile. When the lateral load H_0 = 500 kN, the position of the soil resistance zero point of the pile for the level ground appears at 4.36 m below the ground surface, while that for the slope ratio of 1V : 1H appears at 5.09 m. More soil is needed to provide lateral soil resistance to balance the interaction between pile and soil due to the reduction of soil volume in front of the pile.

(4) The soil resistance increases in the opposite direction near the bottom of the pile for higher load levels. This could be due to the fact that the large deformation of the pile makes the embedded part of the pile to cause a certain lateral displacement and separate from the soil around the pile, resulting in tension stress of soil. In addition, the soil resistance will increase in the opposite direction near the bottom of the pile as the slope ratio increases for the same load level.

3.2. Effect of Loading Direction. For the pile adjacent to the slope under lateral load, the conditions of soil in front of the pile and the soil behind the pile will directly affect the bearing mechanism of the pile. The conditions of soil in front of the pile and the soil behind the pile are asymmetrical. The lack of soil mass on the slope side of the pile tends to reduce the bearing capacity of the pile. Therefore, the loading directions (toward loading and reverse loading) have different effects on the pile bearing mechanism (Figure 14).

In order to study the bearing mechanism of the pile under different loading directions, the pile distance from slope crest B/D of different models was set as 1, 3, 5, 7, and ∞ (level ground), respectively, with the slope ratio of 1V : 1H. Toward lateral load and reverse lateral load were applied on the models for comparative analysis. To simplify the presentation of results, TL is toward loading in short and RL is reverse loading in short. The pile displacement, bending moment, and lateral soil resistance for reverse loading are all positive values.

Figure 15 shows the contours of lateral displacement of the pile and soil for the 1V : 1H slope at a lateral load of 1000 kN with different loading directions. It can be seen from the figure that the loading directions (toward loading and reverse loading) affect the lateral displacement field of the soil before the pile. The displacement field of the soil in the shallow foundation for forward loading is distributed in the shape of wedge, while that for reverse loading is distributed in the U-shaped area. The maximum displacement for forward loading is much larger than that for reverse loading, which indicates that the loading direction has a great influence on the bearing mechanism of the pile adjacent to a slope.

The pile head load-displacement curves are shown in Figure 16 under different loading directions for the 1V : 1H slope. It can be seen that, with the increase of lateral load, the pile head displacement increases rapidly. The curves for toward loading are quite different, while the curves for reverse loading are very similar. It indicates that the pile head displacement is significantly affected by the pile distance from slope crest under toward loading. On the contrary, the pile distance from slope crest under reverse loading has little effect on the pile head displacement. The maximum pile head displacement is 298.813 mm under toward lateral loading of 1000 kN, while the maximum pile head displacement is only 118.543 mm under reverse lateral loading of the same load level, which demonstrates that reverse loading is not conducive to the development of pile head displacement.

Figures 17 and 18 show the variation of lateral pile deflection with depth for the 1V : 1H slope under different loading directions at lateral loads of 500 kN and 1000 kN, respectively. The findings from Figures 17 and 18 can be listed as follows:

(1) When H_0 = 500 kN, the maximum pile displacement under reverse lateral loading increases by 6.61% from B/D = 7 to B/D = 1. In the meanwhile, the position of the first displacement zero point moves downward from 5.49 m to 6.01 m with the decrease of pile distance from slope crest. This is because the critical load values are different for soil around the pile with different B/D to change from elastic deformation to plastic deformation at lower applied load levels. The soil that first enters the plastic deformation causes the pile to have a larger deflection and also expands the plastic zone into the deeper foundation soil.

(2) When the lateral load increases to 1000 kN, the maximum pile displacement under reverse lateral loading only increases by 4.24% from B/D = 7 to B/D = 1. In addition, the position of the first displacement zero point for different B/D is about 6.01 m below the

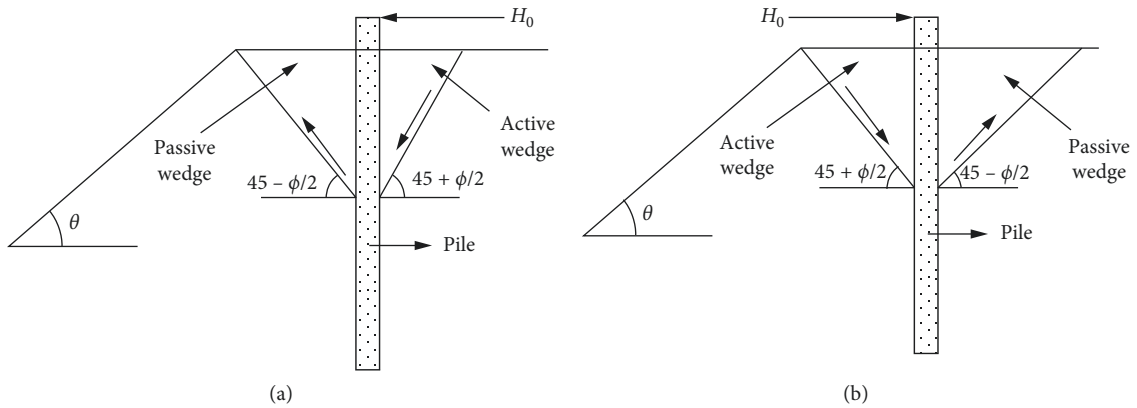

Figure 14: Failure mechanism of a pile in sloping ground. (a) Toward loading. (b) Reverse loading.

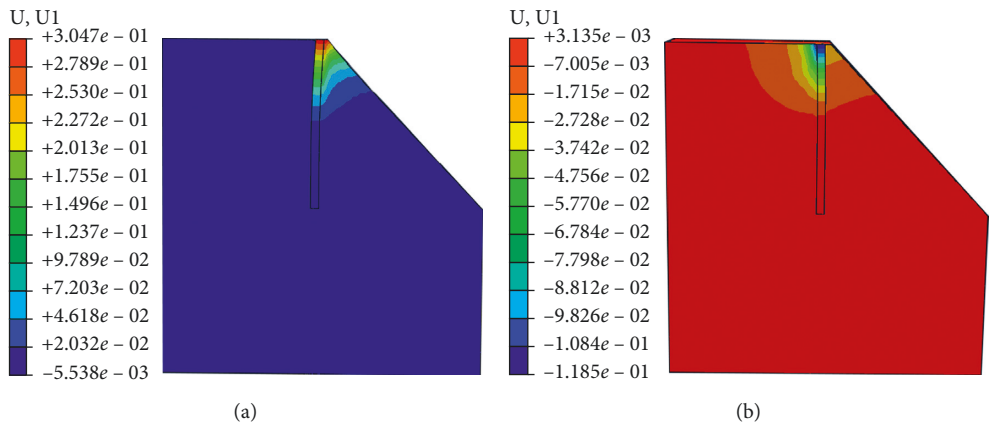

Figure 15: Lateral displacement field at H_0 = 1000 kN for the 1V : 1H slope. (a) Toward loading. (b) Reverse loading.

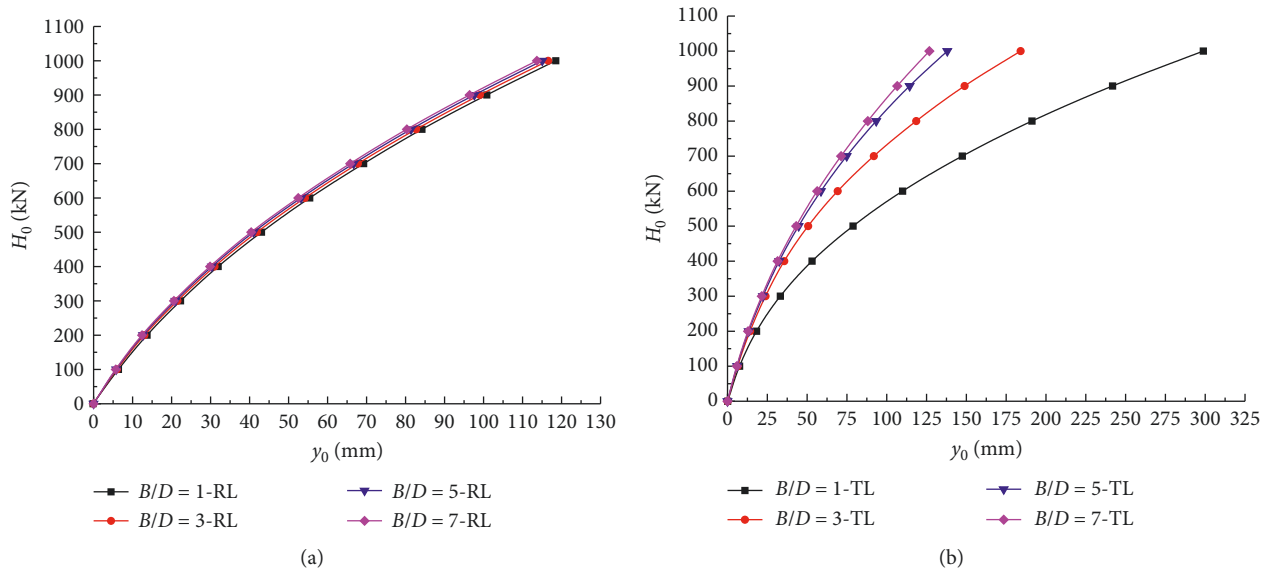

Figure 16: Pile head load-displacement curves under different loading directions for the 1V : 1H slope. (a) Reverse loading. (b) Toward loading.

ground surface. It indicates that when the lateral load increases to a certain critical value, the soil around the pile for different B/D has completely entered the stage of plastic deformation and pile displacement gradually increases to the maximum value and no longer changes.

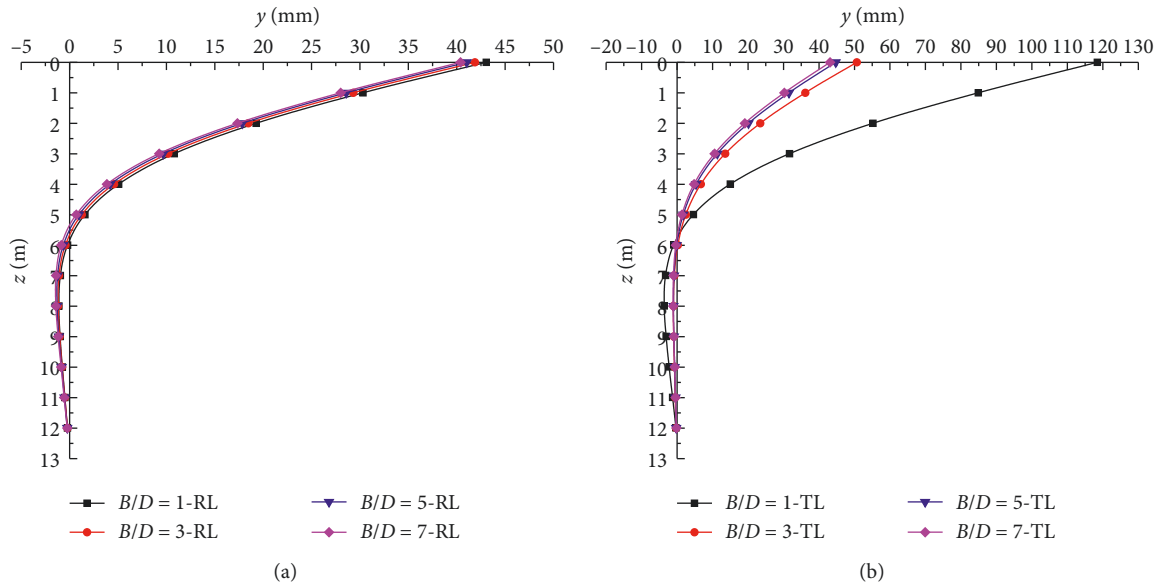

FIGURE 17: Pile deflection versus depth relationships under different loading directions for the 1V : 1H slope at H_0 = 500 kN. (a) Reverse loading. (b) Toward loading.

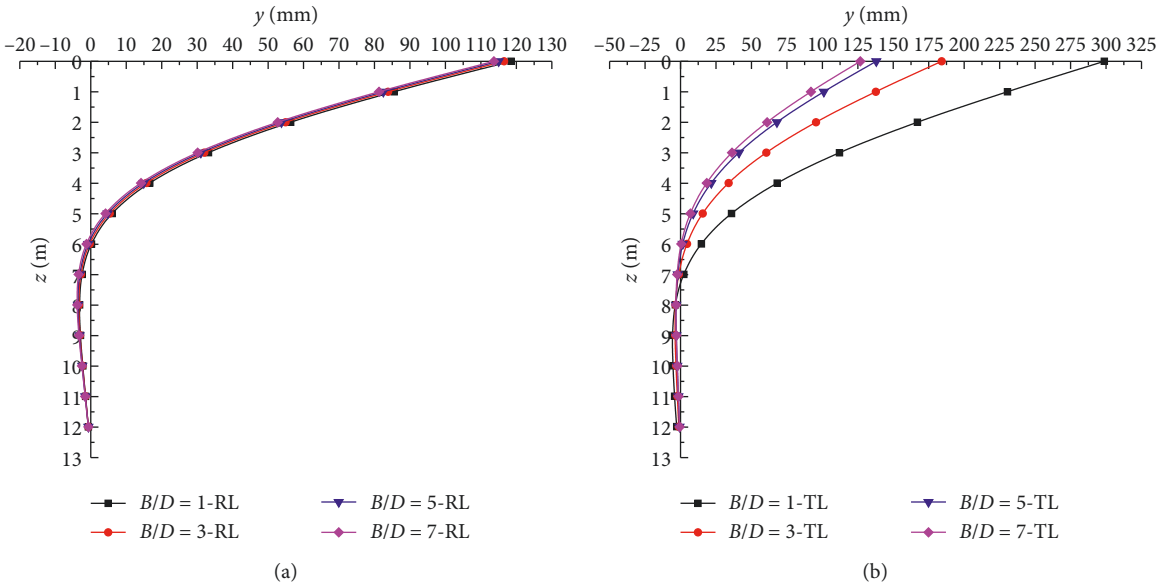

FIGURE 18: Pile deflection versus depth relationships under different loading directions for the 1V : 1H slope at H_0 = 1000 kN. (a) Reverse loading. (b) Toward loading.

(3) The pile deflection is greatly affected by the pile distance from slope crest. Moreover, the increase of pile deflection will become greater as the load level increases.

The variation of bending moment with depth for the 1V : 1H slope under different loading directions with different B/D is presented in Figure 19. From Figure 19, these findings can be drawn:

(1) As the lateral load increases, the bending moment of the pile under different loading directions increases. However, the bending moment of the pile for reverse loading is lower than that for toward loading under the same condition. It indicates that the bearing capacity of the pile for reverse loading is better than that for toward loading due to the fact that the passive wedge for toward loading is near the slope.

(2) With the increase of pile distance from slope crest, the bending moment of the pile for reverse loading gradually approaches the bending moment of the pile for toward loading. Moreover, when the pile distance from slope crest increases to a critical value, the effect of loading direction on the bending moment of the

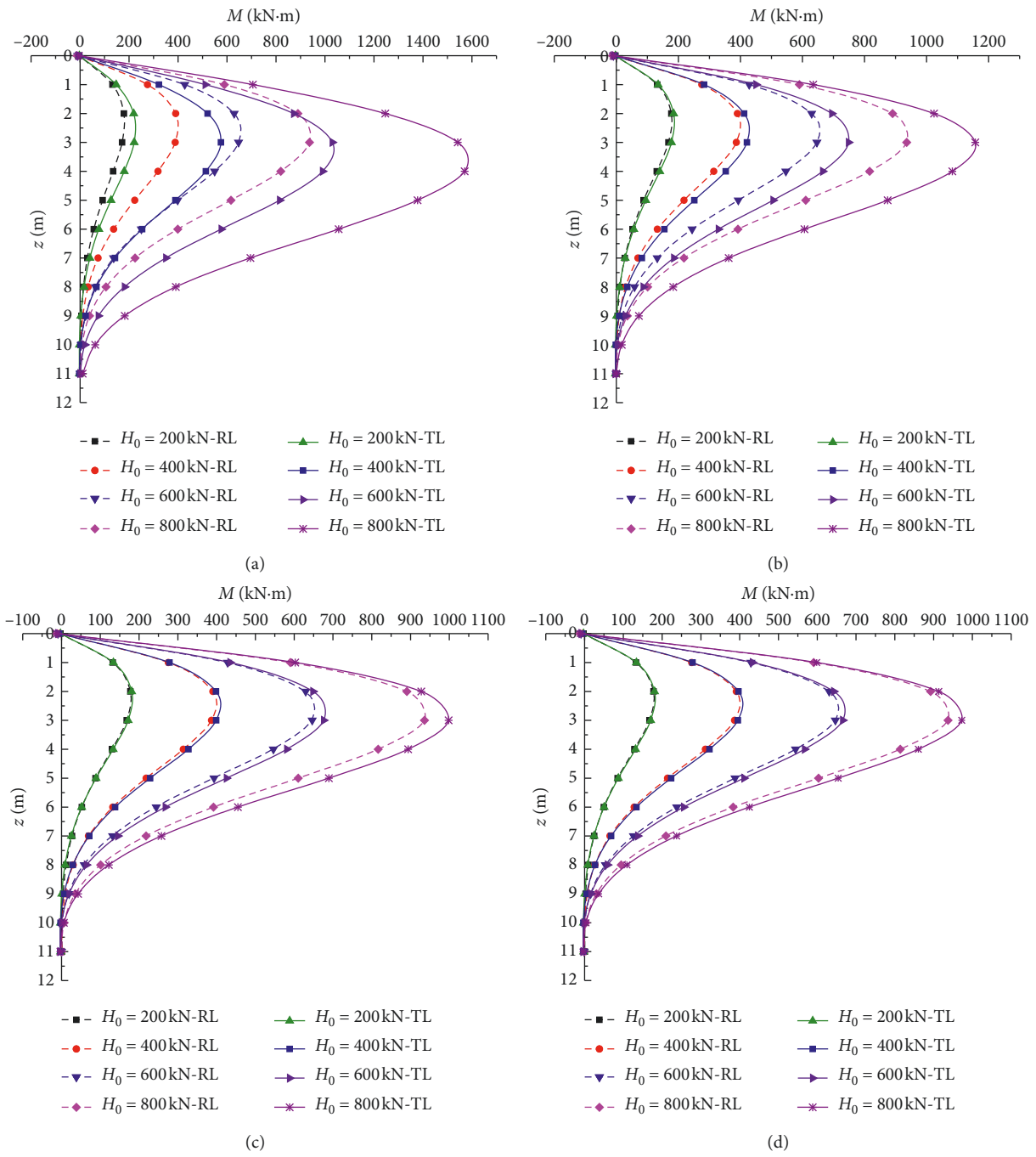

Figure 19: Bending moment of the pile versus depth relationships under different loading directions for the 1V : 1H slope. (a) $B/D = 1$. (b) $B/D = 3$. (c) $B/D = 5$. (d) $B/D = 7$.

pile can be neglected. At an applied load $H_0 = 800$ kN, the maximum bending moment of the pile for reverse loading is 40.32% lower than that for toward loading with $B/D = 1$. When the pile distance from slope crest B/D increases to 7, the maximum bending moment of the pile for reverse loading is only 2.5% lower than that for toward loading.

(3) The position of the maximum bending moment of the pile for reverse loading is higher than that for toward loading at the same load level with small B/D. The effect of loading direction on the position of the bending moment of the pile becomes smaller as the pile distance from slope crest increases. When the pile distance from slope crest B/D increases to 7, the positions of the bending moment of the pile for different loading directions are the same.

Figures 20 and 21 show the curves of lateral soil resistance under different loading directions for the 1V : 1H slope at $H_0 = 500$ kN and $H_0 = 1000$ kN, respectively. It can be seen that the soil resistance on the ground surface for

reverse loading is higher than that for toward loading at the same load level and B/D. In addition, the soil resistance values for reverse loading are almost the same, while those for toward loading are very obvious. It indicates that the slope has little effect on the soil resistance for reverse loading because of the integrity of soil in front of the pile for reverse loading.

The position of the soil resistance zero point of the pile for reverse loading is higher than that for toward loading at the same load level. When the lateral load $H_0 = 500$ kN, the position of the soil resistance zero point of the pile for reverse loading appears at 4.29~4.33 m below the ground surface, while that for toward loading appears at 4.35~5.1 m. The pile deflection becomes greater when the position of the soil resistance zero point of the pile gets deeper. Therefore, the pile under reverse loading is safer than the pile under toward loading under the same conditions.

4. Conclusions

In order to further explore the bearing mechanism of the laterally loaded single pile in clay slope under different working conditions, this paper uses the finite element software to establish the laterally loaded pile in sloping ground considering the slope ratio and loading direction. Based on the results of finite element calculation from different numerical models, the following main conclusions can be drawn:

(1) According to the data from previous works, a three-dimensional finite element verification model of the undrained lateral pile in sloping ground was established. By comparing the finite element results with the theoretical calculation results, the correctness of the three-dimensional finite element modeling method was proved.

(2) The slope causes greater pile deflection and internal force compared with level ground. The growth rate of pile head displacement and maximum bending moment is much larger with the increase of lateral load as the slope gets steeper. In the meanwhile, the increase of the slope ratio will also cause the position of maximum bending moment and soil resistance zero point of the pile to move downward, further increasing the pile deflection.

(3) When the pile distance from slope crest $B < 7D$, regardless of the loading direction, the compressive soil in front of piles is affected by the slope effect, thus affecting the bearing characteristics of the pile foundation. The displacement and internal force development of the pile under toward loading is more obvious. Moreover, when the pile distance from slope crest exceeds 7D, the effect of loading direction on the pile can be neglected.

Data Availability

Readers can get the data from the numerical simulation mentioned in this paper. Finite element models were created with appropriate model sizes, and reasonable model parameters were assigned for numerical calculations. From the calculation results, the data in the software were extracted, which were processed by the software Origin to obtain diagrams in the paper. Because the data extracted from the software were useful, there were no unavailable data. In addition, the data used to support the findings of this study are available from the corresponding author upon request.

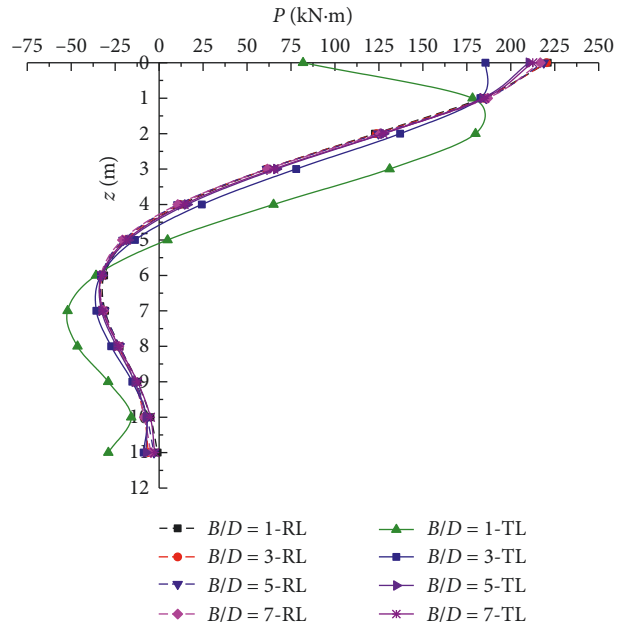

Figure 20: Lateral soil resistance versus depth relationships under different loading directions for the 1V : 1H slope at $H_0 = 500$ kN.

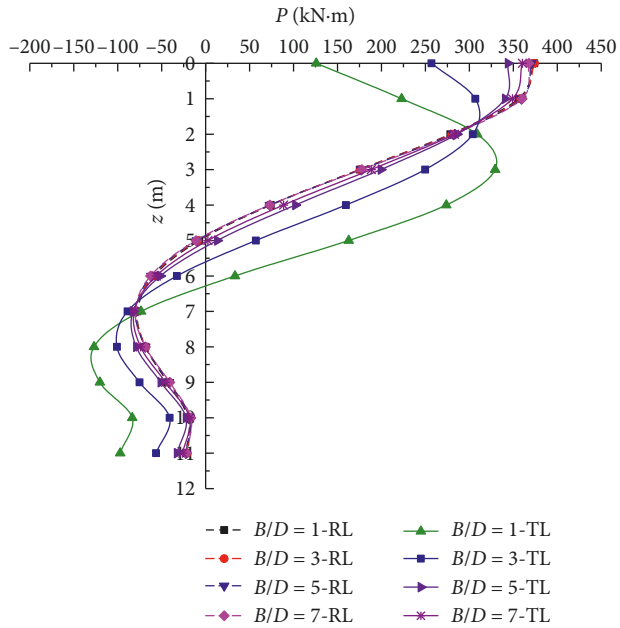

Figure 21: Lateral soil resistance versus depth relationships under different loading directions for the 1V : 1H slope at $H_0 = 1000$ kN.

Conflicts of Interest

The authors declare that there are no conflicts of interest regarding the publication of this paper.

Acknowledgments

This work was supported by the National Natural Science Foundation of China (Grant Nos. 51478479 and 51678570) and Hunan Transport Technology Project (Grant No. 201524).

References

[1] K. Georgiadis, M. Georgiadis, and C. Anagnostopoulos, "Lateral bearing capacity of rigid piles near clay slopes," *Soils and Foundations*, vol. 53, no. 1, pp. 144–154, 2013.

[2] L. C. Reese, W. M. Isenhower, and S. T. Wang, *Analysis and Design of Shallow and Deep Foundations*, Blackwell Science Publishing, Hoboken, NJ, USA, 2006.

[3] D. P. Stewart, "Reduction of undrained lateral pile capacity in clay due to an adjacent slope," *Australian Geomechanics*, vol. 34, no. 4, pp. 17–23, 1999.

[4] K. Bhushan, S. C. Haley, and P. T. Fong, "Lateral load tests on drilled piers in stiff clays," *Journal of the Geotechnical Engineering Division-ASCE*, vol. 105, no. 8, pp. 969–985, 1979.

[5] A. D. Mirzoyan and K. M. Rollins, "Full scale tests to evaluate lateral pile resistance at the edge of a slope," in *Proceedings of 32nd Annual Conference on Deep Foundations, DFI*, Colorado Springs, CO, USA, 2007.

[6] A. D. Mirzoyan, "Lateral resistance of piles at the crest of slope in sand," M. S. thesis, Brigham Young University, Provo, Utah, 2007.

[7] H. G. Poulos, "Behavior of laterally loaded piles near a cut or slope," *Australian Geomechanics Journal*, vol. 6, no. 1, pp. 6–12, 1976.

[8] S. V. Sivapriya and S. R. Gandhi, "Experimental and numerical study on pile behavior under lateral load in clayey slope," *Indian Geotechnical Journal*, vol. 43, no. 1, pp. 105–114, 2013.

[9] S. Mezazigh and D. Levacher, "Laterally loaded piles in sand: slope effect on P-Y reaction curves," *Canadian Geotechnical Journal*, vol. 35, no. 3, pp. 433–441, 1998.

[10] K. Muthukkumaran, "Effect of slope and loading direction on laterally loaded piles in cohesionless soil," *International Journal of Geomechanics*, vol. 14, no. 1, pp. 1–7, 2014.

[11] N. Nimityongskul, Y. Kawamata, D. Rayamajhi, and S. A. Ashford, "Full-scale tests on effects of slope on lateral capacity of piles installed in cohesive soils," *Journal of Geotechnical and Geoenvironmental Engineering*, vol. 144, no. 1, article 4017103, 2018.

[12] D. A. Brown and C.-F. Shie, "Some numerical experiments with a three dimensional finite element model of a laterally loaded pile," *Computers and Geotechnics*, vol. 12, no. 2, pp. 149–162, 1991.

[13] K. Georgiadis and M. Georgiadis, "Undrained lateral pile response in sloping ground," *Journal of Geotechnical and Geoenvironmental Engineering*, vol. 136, no. 11, pp. 1489–1500, 2010.

[14] C. W. W. Ng and L. M. Zhang, "Three-dimensional analysis of performance of laterally loaded sleeved piles in sloping ground," *Journal of Geotechnical and Geoenvironmental Engineering*, vol. 127, no. 6, pp. 499–509, 2001.

[15] L. M. Zhang, C. W. W. Ng, and C. J. Lee, "Effects of slope and sleeving on the behavior of laterally loaded piles," *Soils and Foundations*, vol. 44, no. 4, pp. 99–108, 2004.

[16] V. A. Sawant and S. K. Shukla, "Effect of edge distance from the slope crest on the response of a laterally loaded pile in sloping ground," *Geotechnical and Geological Engineering*, vol. 32, no. 1, pp. 197–204, 2014.

[17] R. Baker, "A second look at Taylor's stability chart," *Journal of Geotechnical and Geoenvironmental Engineering*, vol. 129, no. 12, pp. 1102–1108, 2003.

[18] L.-Y. Xu, F. Cai, G.-X. Wang, and K. Ugai, "Nonlinear analysis of laterally loaded single piles in sand using modified strain wedge model," *Computers and Geotechnics*, vol. 51, pp. 60–71, 2013.